TWO ENERGY-BASED DAMAGE DESCRIPTIONS TO PREDICT FATIGUE LIFE OF STEEL SAMPLES SUBJECTED TO MULTIAXIAL LOADING SPECTRA

[1]G.R.AHMADZADEH, [2]A.VARVANI-FARAHANI

[1,2]Postdoctoral fellow, Professor of Department of Mechanical Engineering, Ryerson University,
350 Victoria Street, Toronto, Ontario M5B 2K3
E-mail: [1]reza.ahmadzadeh@ryerson.ca, [2]avarvani@ryerson.ca

Abstract - Two energy-based models of Varvani-Farahani (VF) and Łagoda-Macha (LM) are employed to evaluated Fatigue life of different steel alloys subjected to irregular non proportional loading paths. The VF model assessed fatigue life through summation of both ranges of normal and shear energy on the critical plane. These ranges are determined from the largest stress and strain Mohr's circles over the counted loading and unloading reversals. LM damage model evaluated the life of samples based on the equivalent strain energy densities over reversals of the applied stress and strain histories on the critical plane. The reversals over loading histories were counted by means of the equivalent relative strain method of the Wang-Brown. Damage values were calculated for each counted reversal and then accumulated based on the Miner-Palmgren linear damage rule. Fatigue life is calculated from the overall damage based on two damage models. As predicted lives based on these damage models compared with those of reported experimental data showed that estimated lives based on VF model have a better agreement.

Index Terms - Critical plane criteria, Cycle counting, Fatigue Life prediction, Irregular nonproportional path.

I. INTRODUCTION

In design of engineering components and structures such as pressure vessels, turbines, airframes and landing gears undergoing irregular loading special attentions is required to increase service safety and to prevent mechanical failure as well as to reduce the cost of maintenance. It is crucial to develop effective models to assess fatigue life under complex states of stress and strain [1]. For the evaluation of fatigue life of components under multiaxial loading conditions, different approaches have been implemented. Various damage criteria on the basis of strain energy density on the critical plane have been developed by many researchers [2-11].

In this approach, fatigue damage assessment involves components of stress and strain on the critical plane to address the shortcomings of earlier developed strain-based and stress–based models. Smith-Watson-Topper (SWT) [3] developed simple equation multiplying applied strain amplitude and maximum stress. Liu [5] proposed virtual strain energy model based on the elastic and plastic work components. Chu et al. [2] modified this model to include the influence of mean stress using maximum stress instead of stress range. Glinka et al. [6] employed maximum normal and shear stress to account for the mean stress effect on crack growth. The normal stress on the critical plane was responsible to open the crack and the maximum shear stress to overcome any sliding friction occurring between the crack surfaces. Łagoda and Macha [11] developed a criterion based on the maximum shear and normal stresses in the fracture plane. For multiaxial stress cycles, the equivalent stress history is employed to assess fatigue damage over high-cycle fatigue region [12]. Łagoda and Macha further developed generalized criterion on the maximum shear and normal strain energy density parameter on the critical plane [11]. They verified proposed stress-based criteria to estimate fatigue life of 30CrNiMo8 steel alloy under multiaxial random loading. Lives were predicted within the scatter band of factor 3 [12]. They also calculated fatigue life data of steel alloys under uniaxial and multiaxial random loading conditions using energy-based model [11, 13-16]. Varvani-Farahani [10] proposed a damage model integrating normal and shear strain energy ranges determined from stress and strain components acting on the critical plane. The model was employed to assess life of various materials under uniaxial and multiaxial loading spectra by several researchers. Han et al. [17] employed VF model to assess fatigue life of SNCM630 steel alloy under proportional and non-proportional loading conditions. Their predicted life data fell within factor 2. Chen et al. [18] utilized VF damage model to evaluate fatigue life of Al 7050-T7451 and En15R steel alloys under combined tension-torsion variable loading histories and reported the predicted values fall within the scatter band of factor 2 as compared with experimental data. In a recent paper [19] fatigue damage and life of steel samples subjected to random loading conditions were evaluated based on the SWT, Ellyin, LM and VF damage models with different energy-based descriptions. Fatigue lives based on VF and LM tightly fell in agreement with those of experimental

data as compared with two other damage models. Fatigue life of steel alloys subjected to multiaxial irregular loading paths based on critical plane-energy based damage descriptions developed earlier by Varvani and Łagoda and Macha (LM) is investigated. Wang-Brown Multiaxial cycle-counting is employed to determine the number of reversals acting on the critical plane over peak-valley events of the loading spectrum. Lagoda and Macha proposed equivalent energy parameter to include the normal and shear strain energy densities in the critical plane and the direction of this plane is evaluated based on the weight function method. While, VF model related fatigue damage to life of steel alloys through components of normal and shear stress/strain acting on the critical plane. The choice of damage approaches are discussed based on the stress/strain components they hold and their degree of complexity and consistency in damage assessment.

II. DESCRIPTION OF MODELS

A. Varvani-Farahani Damage Model

An energy-based model was developed to assess fatigue damage of materials based on ranges of the normal and shear stress/strain components acting on the critical plane [10]. These ranges were defined by means of the largest Mohr's circles over loading and unloading reversals (peak-valley events) of the loading spectrum. The energy components in VF model [10, 20] consisted of the product of the normal stress and strain ranges $\Delta\sigma_n\Delta\varepsilon_n$ and the product of shear stress and strain ranges $\Delta\tau_{\max}\Delta(\gamma/2)_{\max}$ acting on the critical plane as:

$$W_{VF}=\frac{1}{\sigma_f'\varepsilon_f'}\left(\Delta\sigma_n\Delta\varepsilon_n\right)+\frac{1}{\tau_f'\gamma_f'}\left(\Delta\tau_{\max}\left(\frac{\Delta\gamma}{2}\right)_{\max}\right)$$
$$=\left[\frac{\sigma_f'}{E}\left(N_f\right)^b+\varepsilon_f'\left(N_f\right)^c\right]+\left[\frac{\tau_f'}{G}\left(N_f\right)^{b_0}+\gamma_f'\left(N_f\right)^{c_0}\right] \quad (1)$$

Both normal and shear energy components were weighted by tensile and shear fatigue properties. In the right hand side of this equation, the overall damage over peak-valley events of a loading spectrum was related to fatigue life N_f based on Coffin-Manson type equations [21] including tensile and shear moduli (E and G), tensile and shear fatigue strength coefficients (σ_f' and τ_f') and tensile and shear fatigue ductility coefficients (ε_f' and γ_f'), and exponents (b, c and b_0, c_0). Based on the largest the strain and stress Mohr's circles during loading (L) and unloading (UL) reversals, the ranges of maximum shear strain/stress and the corresponding normal strain/stress ranges on the critical plane are calculated as:

$$\Delta\left(\frac{\gamma}{2}\right)_{\max}=\left(\frac{\varepsilon_1-\varepsilon_3}{2}\right)_L-\left(\frac{\varepsilon_1-\varepsilon_3}{2}\right)_{UL} \quad (2a)$$

$$\Delta\tau_{\max}=\left(\frac{\sigma_1-\sigma_3}{2}\right)_L-\left(\frac{\sigma_1-\sigma_3}{2}\right)_{UL} \quad (2b)$$

$$\Delta\varepsilon_n=\left(\frac{\varepsilon_1+\varepsilon_3}{2}\right)_L-\left(\frac{\varepsilon_1+\varepsilon_3}{2}\right)_{UL} \quad (2c)$$

$$\Delta\sigma_n=\left(\frac{\sigma_1+\sigma_3}{2}\right)_L-\left(\frac{\sigma_1+\sigma_3}{2}\right)_{UL} \quad (2d)$$

where ε_1, ε_2, ε_3 and σ_1, σ_2, σ_3 are the principal strain and stress values ($\varepsilon_1>\varepsilon_2>\varepsilon_3$ and $\sigma_1>\sigma_2>\sigma_3$).

VF model was employed to assess damage over counted reversals and damage of reversals over block loading history was accumulated to evaluate the number of blocks to failure in steel samples.

B. Łagoda-Macha Damage Model

Macha developed an energy-based criterion [11, 14-16] to assess fatigue life in low- and high-cycle fatigue regimes based on the components of maximum normal and shear energy densities defined on the critical plane:

$$\max\left\{\beta W_{ns}(t)+\kappa W_n(t)\right\}=Q \quad (3)$$

The orientation of critical plane is normal to the mean direction along with maximum principal stress. The plane was identified by the unit normal vector $\bar{n}$ coinciding with the mean direction of stress $\bar{s}$. The mean direction coincided with the maximum shear strain energy density $W_{ns}(t)$ and the normal energy density $W_n(t)$ occurred along unit normal vector $\bar{n}$. the coefficients β and κ in equation (1) represent material constants and are evaluated respectively based on $\beta=2/(1+\nu)$ and $\kappa=2/(1-\nu)$.

The short form of left hand side of equation (1) is presented as $\max\{W_{eq}(t)\}$ and fatigue fracture occurs when maximum value of $W_{eq}(t)$ exceeds uniaxial fatigue limit Q. Kardas et al. [15] determined the equivalent energy parameter $W_{eq}(t)$ based on the mean direction cosines of principal stress/strain, $\hat{l}_n,\hat{m}_n,\hat{n}_n$ (where n=1, 2, 3) to as:

$$W_{eq}(t)=\frac{2}{(1+\nu)}\left[\tau_{ns}(t)\left|\gamma_{ns}(t)\right|+\left|\tau_{ns}(t)\right|\gamma_{ns}(t)\right]+\frac{2}{(1-\nu)}\left[\sigma_n(t)\left|\varepsilon_n(t)\right|+\left|\sigma_n(t)\right|\varepsilon_n(t)\right] \quad (4)$$

where $\tau_{ns}(t)$ is maximum shear stress, $\gamma_{ns}(t)$ represents maximum shear strain, $\sigma_n(t)$ and $\varepsilon_n(t)$ are respectively maximum normal stress and maximum normal strain on the critical plane. The maximum shear stress on the critical plane is evaluated as:

$$\tau_{ns}(t)=\frac{\hat{l}_1^2-\hat{l}_3^2}{2}\sigma_{xx}(t)+\frac{\hat{m}_1^2-\hat{m}_3^2}{2}\sigma_{yy}(t)+\frac{\hat{n}_1^2-\hat{n}_3^2}{2}\sigma_{zz}(t)+\left(\hat{l}_1\hat{m}_1-\hat{l}_3\hat{m}_3\right)\tau_{xy}(t)$$
$$+\left(\hat{l}_1\hat{n}_1-\hat{l}_3\hat{n}_3\right)\tau_{xz}(t)+\left(\hat{m}_1\hat{n}_1-\hat{m}_3\hat{n}_3\right)\tau_{yz}(t) \quad (5a)$$

In above equation, terms σ_{ij} and τ_{ij} (where i,j=x,y,z) represent axial and shear stresses in the direction of x,y and z. Garud cyclic plasticity hardening rule [15] was employed to calculate the magnitude of stress at any given strain values over loading spectra. The maximum shear strain on the critical plane is defined as:

$$\gamma_{ns}(t)=\frac{1}{2}\left[\left(\hat{l}_1^2-\hat{l}_3^2\right)\varepsilon_{xx}(t)+\left(\hat{m}_1^2-\hat{m}_3^2\right)\varepsilon_{yy}(t)+\left(\hat{n}_1^2-\hat{n}_3^2\right)\varepsilon_{zz}(t)+\left(\hat{l}_1\hat{m}_1-\hat{l}_3\hat{m}_3\right)\gamma_{xy}(t)\right.$$
$$\left.+\left(\hat{l}_1\hat{n}_1-\hat{l}_3\hat{n}_3\right)\gamma_{xz}(t)+\left(\hat{m}_1\hat{n}_1-\hat{m}_3\hat{n}_3\right)\gamma_{yz}(t)\right]$$

(5b)

The maximum normal stress on the critical plane is defined as:

$$\sigma_n(t)=\hat{l}_1^2\sigma_{xx}(t)+\hat{m}_1^2\sigma_{yy}(t)+\hat{n}_1^2\sigma_{zz}(t)+2\hat{l}_1\hat{m}_1\tau_{xy}(t)+2\hat{l}_1\hat{n}_1\tau_{xz}(t)+2\hat{m}_1\hat{n}_1\tau_{yz}(t) \quad (5c)$$

The maximum normal strain on the critical plane is expressed as:

$$\varepsilon_n(t)=\hat{l}_1^2\varepsilon_{xx}(t)+\hat{m}_1^2\varepsilon_{yy}(t)+\hat{n}_1^2\varepsilon_{zz}(t)+2\hat{l}_1\hat{m}_1\gamma_{xy}(t)+2\hat{l}_1\hat{n}_1\gamma_{xz}(t)+2\hat{m}_1\hat{n}_1\gamma_{yz}(t)$$

(5d)

The state of stress/strain is very governing factor to determine the orientation of critical plane. Three different methods of (i) the weight function [22], (ii) the damage accumulation [23] and (iii) the variance method [24] are available to determine the direction of unit vectors $\overline{s}$ and $\overline{n}$. In this paper, the first method was chosen to determine the mean values $\hat{l}_n, \hat{m}_n, \hat{n}_n$. The weight function method takes the average of instantaneous direction of principal stress axes. Based on the directions of principal axes, mean directions of maximum shear stresses are obtained. Details of weight function method and its procedure are given in ref. [22]. The cumulative damage calculated from peak-valley events of block histories in the LM approach is related to fatigue life N_f through Smith-Watson-Topper (SWT) equation in the right hand side of equation (1). The general form of this equation is converted as:

$$\max\left\{W_{eq}(t)\right\}=\frac{\sigma_f'^2}{E}\left(N_f\right)^{2b}+\sigma_f'\varepsilon_f'\left(N_f\right)^{b+c} \quad (6)$$

III. MULTIAXIAL CYCLE COUNTING METHOD

Wang-Brown cycle counting method [1, 25] is employed to evaluate fatigue damage under variable multiaxial loading conditions. The first step in this method is that the equivalent cyclic plastic strain partitions loading spectrum by means of:

$$\varepsilon_{eq}=\frac{1}{\sqrt{2}(1+\nu')}\sqrt{\left(\varepsilon_x-\varepsilon_y\right)^2+\left(\varepsilon_y-\varepsilon_z\right)^2+\left(\varepsilon_x-\varepsilon_z\right)^2+\frac{3}{2}\left(\gamma_{xy}^2+\gamma_{yz}^2+\gamma_{xz}^2\right)} \quad (7)$$

where ν' is the effective Poisson's ratio. This coefficient is determined over peak-valley events of a loading spectrum Based on an iterative process. The maximum value of equivalent strain is identified as the most significant turning point (A). The highest plastic strain in a block is taken as a reference to rearrange data over loading spectrum. The counting process starts calculating the maximum equivalent relative strain with respect to the maximum turning point A as follows:

$$\varepsilon_{eq}^*\left(t=t_E\right)=\max_{A\le t\le end}\varepsilon_{eq}\left(\varepsilon_{ij}(t)-\varepsilon_{ij}^A\right) \quad (8)$$

where t_E is the time at which the new peak takes place at which spectrum data split into two sets. The first set includes increasing data from zero to the maximum point E and another group contains the rest of data. The first group represents one reversal and remaining points are considered to further determine equivalent relative strain and its first peak as the second counted reversal. The counting process is continued over the entire spectrum to count similar points. Details of the procedure of the Wang-Brown cycle counting method and the process of identifying the effective Poisson's ratio have been presented in [26, 27].

IV. MATERIALS AND TESTS

Fatigue damage values and life data of two steel alloys of S45C [28] and S460N [29] tested under various irregular multiaxial loading conditions are employed to predict lives of samples based on the VF and LM damage models. All tests were conducted under strain-controlled condition at room temperature. The details of materials, specimen geometry and fatigue tests were reported in [28, 29]. Table 1 presents fatigue properties of materials employed in the present study.

Material	σ_f' (MPa)	ε_f'	τ_f' (MPa)	γ_f'	b	c	b_0	c_0
S45C [28]	923	0.359	685	0.198	-0.099	-0.519	-0.120	-0.360
S460N [29]	970	0.281	529	0.213	-0.086	-0.493	-0.096	-0.418

Table 1 Fatigue properties of the investigated materials

Multiaxial Strain paths spectra for steel samples are shown in Fig. 1a-1h. This figure shows variation of shear strains versus axial strains. Table 2 lists loading spectra and experimentally obtained fatigue life data for steel alloys studied in this paper. The discretized axial and shear strains at peak-valley events of loading spectra are given in this Table.

Multiaxial loading paths in Fig. 1 and Table 2 include various strain paths of pseudo-random loading (R01 and R02), box (B), constant amplitude out-of-phase (COP), alternating proportional path tests (AP), vertical butterfly (VBF) and horizontal butterfly (HBF).

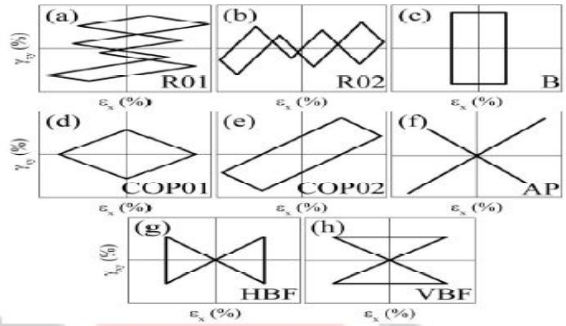


Fig. 1 Multiaxial loading paths for steel alloys S45C with loading paths (a-f) and S460N with strain paths (c), (d), (e), (g) and (h)

Materials	Loading Paths		Strain Peak-Valley events [ε, γ] (%)	N_f (Blocks)
S45C	R	01	[0, 0] [0.4, 0.15] [-0.36, 0.42] [0.16, 0.61] [0.6, 0.45] [-0.4, 0.09] [0.3, -0.17][-0.6, -0.5] [-0.28, -0.61] [0.5, -0.32] [-0.2, -0.07] [0, 0]	936
		02	[0, 0] [0.16, 0.36] [0.46, -0.36] [0.67, 0.15] [0.5, 0.55] [0.1, -0.36] [-0.18, 0.27][-0.54, -0.55] [-0.67, -0.26] [-0.36, 0.48] [-0.08, -0.18] [0,0]	773
	B	-	[0.72, 0.655] [-0.72, 0.655] [-0.72, -0.655] [0.72, -0.655] [0.72, 0.655]	435
	COP	01	[0, -0.545] [0.6, 0] [0, 0.545] [-0.6, 0] [0, -0.545]	1617
		01	[0, -0.409] [0.9, 0] [0, 0.409] [-0.9, 0] [0, -0.409]	678
		02	[0.6, 0.273] [0.3, 0.545] [-0.6, -0.273] [-0.3, -0.545] [0.6, 0.273]	1631
		02	[1.8, 0.614] [1.35, 0.818] [-1.8, -0.614] [-1.35, -0.818] [1.8, 0.614]	215
		02	[1.8, 0.409] [0.9, 0.818] [-1.8, -0.409] [-0.9, -0.818] [1.8, 0.409]	191
	AP	-	[0, 0] [0.8, 0.73] [-0.8, -0.73] [0, 0] [0.8, -0.73] [-0.8, 0.73] [0, 0]	360
		-	[0, 0] [0.8, 0.73] [-0.8, -0.73] [0, 0] [0.6, -0.52] [-0.6, 0.52] [0, 0]	467
S460N	B	-	[0.173, 0.3] [-0.173, 0.3] [-0.173, -0.3] [0.173, -0.3] [0.173, 0.3]	5700
		-	[0.231, 0.4] [-0.231, 0.4] [-0.231, -0.4] [0.231, -0.4] [0.231, 0.4]	4050
		-	[0.144, 0.25] [-0.144, 0.25] [-0.144, -0.25] [0.144, -0.25] [0.144, 0.25]	17950
	COP	01	[0, -0.3] [0.173, 0] [0, 0.3] [-0.173, 0] [0, -0.3]	27000
		01	[0, -0.4] [0.231, 0] [0, 0.4] [-0.231, 0] [0, -0.4]	5935
	HBF	-	[0, 0] [0.173, 0.3] [0.173, -0.3] [-0.173, 0.3] [-0.173, -0.3] [0, 0]	10000
		-	[0, 0] [0.231, 0.4] [0.231, -0.4] [-0.231, 0.4] [-0.231, -0.4] [0, 0]	10450
		-	[0, 0] [0.3, 0.52] [0.3, -0.52] [-0.3, 0.52] [-0.3, -0.52] [0, 0]	1510
	VBF	-	[0, 0] [0.173, 0.3] [-0.173, 0.3] [0.173, -0.3] [-0.173, -0.3] [0, 0]	10050
		-	[0, 0] [0.231, 0.4] [-0.231, 0.4] [0.231, -0.4] [-0.231, -0.4] [0, 0]	8000
		-	[0, 0] [0.3, 0.52] [-0.3, 0.52] [0.3, -0.52] [-0.3, -0.52] [0, 0]	2090

Table 1 Multiaxial strain paths and corresponding fatigue life

V. FATIGUE LIFE PREDICTION RESULTS AND DISCUSSION

Fatigue lives of S45C and S460N steel alloys subjected to various multiaxial irregular loading paths were evaluated based on two energy-based damage models of LM and VF.

Fig. 2 compares the predicted and experimental fatigue lives of S45C steel samples undergoing loading spectra R01, R02, B, COP01, COP02 and AP.

Predicted life data based on both models for loading spectra AP, B, COP01 fell between factors ±2. However the predicted lives for loading spectra R02 and COP02 slightly exceeded ±3 boundaries.

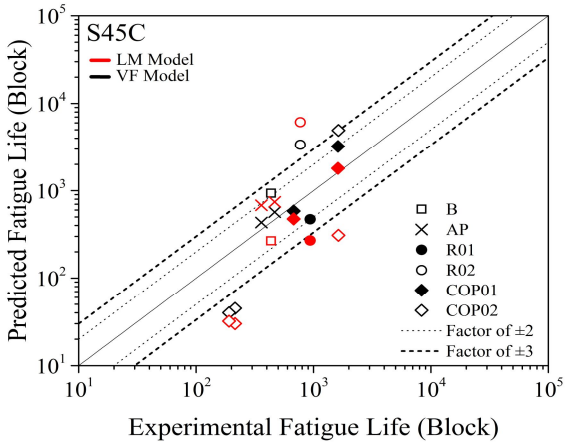


Fig. 2 Predicted versus experimental fatigue lives of S45C steel alloy under various multiaxial loading paths based on the LM and VF damage models

In Fig. 3, the predicted and experimental lives of S460N steel samples subjected to loading histories B, VBF, HBF and COP01 was compared.

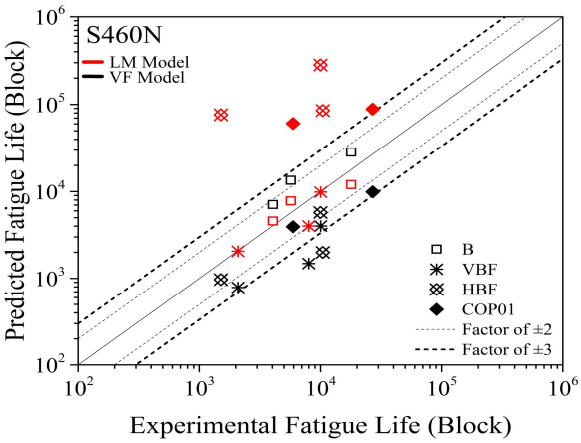


Fig. 3 Predicted versus experimental fatigue lives of S460N steel alloy under various multiaxial loading paths based on the LM and VF damage models

The LM model overpredicted more than 30% of life data beyond factor 3. Over 80% of predicted lives by the VF model collapsed within ±3 factor. LM model predicted 50% of data within scatter band of ±2 while majority of predicted data based on this approach were found non-conservative as compared with experimental data. Fig. 4 plots collectively the predicted fatigue life data based on LM and VF models versus experimental data of S45C and S460N steel samples under various multiaxial loading conditions. This figure compares predicted life data based on LM approach (open symbols) and the predicted life data by VF model (solid symbols). Of twenty one multiaxial fatigue tests, about 50% of fatigue data predicted by VF model fell within ±2 factor, 35% within factor of ±3 and only 15% positions slightly deviates from ±3 bounds. While based on the LM model over 35% of data collapsed within ±2 and remaining data fell within and beyond ±3 bounds.

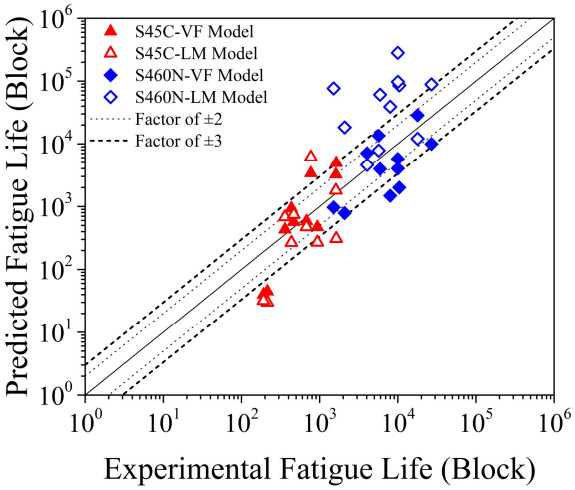


Fig. 4 Predicted versus experimental fatigue lives of S45C and S460N steel alloys under different multiaxial loading conditions based on the LM and VF damage models

The Varvani damage approach through equation (1) however accounted for peak-valley events in overall damage assessment involving the range of stress and strain components acting on the critical plane. The multiaxial reversals at any instance of a loading spectrum held positive or/and negative values. The accumulated damage was calculated through integration of damage over entire block loading spectrum involving both normal and shear stress and strain ranges. Predicted lives based on this model fell tightly below the centerline in fig. 3 for S460N steel alloy. Multiaxial reversals over loading spectra COP02, VBF and HBF in this figure possessed peak-valley events with opposite signs at which the calculated ranges of stress and strain components increased the magnitude of overall damage resulting in a more conservative life prediction based on VF model.

The deviation of LM model from the perfect line of prediction is associated with the fact that the alternative absolute components of maximum shear strain and stress ($\gamma_{ns}(t)$ and $\tau_{ns}(t)$) in the first term of equation (4) and similarly alternative absolute functions of maximum normal strain and stress components ($\varepsilon_n(t)$ and $\sigma_n(t)$) in the second term of this equation produced positive and negative shear and normal energies over peak-valley events caused of reduction of the accumulated damage over a block loading spectrum. Histories R02 in S45C, and COP01 and HBF in S460N steel samples possessed multiaxial reversals at which the product of concurrent positive and negative stress and strain values resulted in negative energies. The difference between positive and negative shear and normal energies achieved over loading instances due to alternative absolute stress/strain values in LM model reduced the accumulated damage largely.

The reduced accumulated damage over peak-valley events then resulted in overprediction of fatigue life data. On the other hand S45C steel samples with loading spectra R01 and COP02 involved multiaxial loading instances at which shear and axial peak-valley events were in opposite sign. The absolute function in equation (4) converted them to positive values resulting in a summation of shear and normal energy terms and an increase in overall damage. The predicted lives for these histories were found more agreeable with the experimental values. Histories R01 and COP02 of S45C steel, and loading paths B and VBF in S460N steel possessed peak-valley events at which absolute components had no influence on the overall damage value. Life prediction of these histories by means of LM model fell within a factor of 2 as compared with experimental data. Fig. 2 presents a relatively close agreements between predicted lives based on both models as compared with those experimental data reported for S45C steel samples. For positive values of stress/strain reversals the absolute functions remained ineffective and the overall damage calculated based on the LM model was found more agreeable with lives predicted based on VF model in this figure. Both models possessed close predicted life values when the products of stress and strain components acting on the critical plane over peak-valley events for this alloy were twice integrated in LM model consistent with ranges of stress/strain components in VF model.

The consistency in the stress and strain ranges over peak-valley events of loading spectra based on VF model has extended the capability of the model to assess fatigue life of steel samples under various multiaxial irregular loading conditions. Overall damage calculated based on LM model through a change in sign of stress and strain terms was highly influenced by loading histories and when loading axes were in-phase reduced the overall damage noticeably and overpredicted fatigue life data.

The non-conservative predicted lives of steel samples by LM model for various multiaxial loading histories (See fig. 4) could also be related to the absence of shear strain and its coefficients in the right hand side of equation (6). The choice of damage assessment models and how to determine the fatigue life of components under irregular loading spectra were attributed to the stress/strain components they possessed, their occurrence, degree of complexity and consistency in damage assessment.

CONCLUSION

Fatigue life of S45C and S460N steel samples tested under various irregular multiaxial loading conditions were predicted based on the LM and VF energy-based models. Majority of the predicted fatigue life data fell within factor ±3 as compared with experimental data. The predicted lives by the LM model consistently showed a non-conservative response while predicted life data by the VF model fell within factor ±3 or better with the conservative response. The LM fatigue damage model held SWT relation in the right hand side of equation (6) relating the overall damage to fatigue life.

The involvement of stress/strain sign over counted reversals in equation (4) as well as the lack of shear strain and coefficients in the right hand side of equation (6) resulted in smaller values of damage calculated over loading spectrum. This noticeably increased the values of predicted lives based on the LM approach. The Varvani model however due to holding ranges of stress/ strain components over counted reversals of block loading histories as well as contribution of shear strain and coefficients in the right hand side of equation (1) enabled a closer agreement with the predicted life data as compared with experimental values.

ACKNOWLEDGEMENTS:

Authors wish to acknowledge the financial support by the Natural Sciences and Engineering Research Council (NSERC) of Canada

REFERENCES

[1] C.H. Wang and M.W. Brown, “Life prediction techniques for variable amplitude multiaxial fatigue – part 1: theories,” Journal of Engineering Materials and Technology, vol. 118, pp.367–70, 1996.

[2] C.C. Chu, F.A. Conle and J.J.F. Bonnen, “Multiaxial stress–strain modeling and fatigue life prediction of SAE axle shafts. In: Advances in Multiaxial Fatigue, ASTM STP 1191, pp. 37–54, 1993.

[3] R.N. Smith, P. Watson and T.H. Topper, “A stress–strain function for the fatigue of metals. Journal of Materials, vol. 5, no. 4, pp.767–78, 1970.

[4] Nitta, T. Ogata and K. Kuwabara, “Fracture mechanisms and life assessment under high-strain biaxial cyclic loading of type 304 stainless steel,” Fatigue & Fracture of Engineering Materials & Structures, vol.12, no. 2, pp.77–92, 1989.

[5] K.C. Liu, “A method based on virtual strain energy parameters for multiaxial fatigue life prediction,” In: Advances in Multiaxial Fatigue, ASTM STP 1191, pp. 67–84, 1993.

[6] G. Glinka, G. Shen and A. Plumtree, “Mean stress effect in multiaxial fatigue,” Fatigue & Fracture of Engineering Materials & Structures, vol. 18, pp. 755–64, 1995.

[7] W.F. Pan, C.Y. Hung and L.L. Chen, “Fatigue life estimation under multiaxial loading,” International Journal of Fatigue, vol. 21, pp. 3–10, 1999.

[8] E. Macha and A. Niesłony, “Critical plane fatigue life models of materials and structures under multiaxial stationary random loading: The state-of-the-art in Opole Research Centre CESTI and directions of future activities,” International Journal of Fatigue, vol. 39, 95–102, 2012.

[9] X. Chen, S. Xu and D. Huang, “A critical plane-strain energy density criterion for multiaxial low-cycle fatigue life under non-proportional loading,” Fatigue & Fracture of Engineering Materials & Structures, vol. 22, pp. 679–86, 1999.

[10] Varvani-Farahani, “A new energy-critical plane parameter for fatigue life assessment of various metallic materials subject to in-phase and out-of-phase multiaxial fatigue loading conditions,” International Journal of Fatigue, vol. 22, pp.295–305, 2000.

[11] T. Łagoda and E. Macha, "Generalization of energy–based multiaxial fatigue criteria to random loading," In: S. Kalluri, P.J. Bonacuse, editors, multiaxial fatigue and deformation: testing and prediction, ASTM STP 1387. West Conshohocken, PA, ASTM, 2000, pp. 173–90.
[12] T. Łagoda and E. Macha, "Estimated and experimental fatigue lives of 30CrNiMo8 steel under in- and out-of-phase combined bending and torsion with variable amplitudes," Fatigue & Fracture of Engineering Materials & Structures, vol. 17, no. 11, pp. 1307–1318, 1994.
[13] T. Łagoda, E. Macha, and W. Będkowski, "A critical plane approach based on energy concepts: Application to biaxial random tension-compression high-cycle fatigue regime," International Journal of Fatigue, vol. 21, pp. 431-443, 1999.
[14] T. Łagoda and P. Ogonowski, "Criteria of multiaxial random fatigue based on stress, strain and energy parameters of damage in the critical plane," Mat.-wiss. u. Werkstofftech, vol. 36, no. 9, pp. 429-437, 2005.
[15] D. Kardas, K. Kluger, T. Łagoda and P. Ogonowski, "Fatigue life of 2017(a) aluminum alloy under proportional constant-amplitude bending with torsion in energy approach," Materials Science, vol. 44, no. 4, pp. 541-549, 2008.
[16] K. Walat, M. Kurek, P. Ogonowski and T. Łagoda, "The multiaxial random fatigue criteria based on strain and energy damage parameters on the critical plane for low-cycle range," International Journal of Fatigue, vol. 37, pp.100-111, 2012.
[17] C. Han, X. Chen and K.S. Kim, "Evaluation of multiaxial fatigue criteria under irregular loading," International Journal of Fatigue, vol. 24, pp. 913–922, 2002.
[18] H. Chen, D.G. Shang, Y.J. Tian and J.Z. Liu, "Comparison of multiaxial fatigue damage models under variable amplitude loading," Journal of Mechanical Science and Technology, vol. 26, no.11, pp. 3439-3446, 2012.
[19] N.A. Kadhim, M. Mustafa and A. Varvani-Farahani, "Fatigue life prediction of low-alloy steel samples undergoing uniaxial random block loading histories based on different energy-based damage descriptions," Fatigue & Fracture of Engineering Materials & Structures, vol. 38, pp. 69–79, 2015
[20] Varvani-Farahani, M. Sharma and M.R. Kianoush, "Fatigue damage analysis and life assessment under variable amplitude loading conditions" Materials Science and Engineering A,; vol. 403, pp. 42-47, 2005.
[21] Varvani-Farahani, M.R. Kianoush and M. Sharma, "Fatigue failure assessment of engineering components under service loading conditions. Materials and Design," vol. 28, pp. 575-580, 2007.
[22] E. Macha, "Simulation investigations of the position of fatigue fracture plane in materials with biaxial loads," Materialwiss Werkst Heft 5/89. p. 153–63 [vol. 20 Heft 4/89. p. 132–6].
[23] Karolczuk and E. Macha, "Critical and fracture plane orientations under multiaxial cyclic and random loading," Archives of Civil and Mechanical Engineering, vol. 51, no.3, pp. 415–35, 2004.
[24] W Będkowski, E. Macha and J.L. Robert, "Weber B. Comparison of variance and damage indicator methods for prediction of the fracture plane orientation," In: E. Macha, W. Będkowski, T. Łagoda, editors. Multiaxial fatigue and fracture, ESIS Publ. 25. Oxford: Elsevier, pp. 147–65, 1999.
[25] C.H. Wang and M.W. Brown, "A path-independent parameter for fatigue under proportional and non-proportional loading" Fatigue & Fracture of Engineering Materials & Structures, 16, pp. 1285–98, 1993.
[26] G.R. Ahmadzadeh and A. Varvani-Farahani , "Fatigue life assessment of steel samples under various irregular multiaxial loading spectra by means of two energy-based critical plane damage models," International Journal of Fatigue, vol. 84, pp. 113–121, 2016.
[27] G.R. Ahmadzadeh and A. Varvani-Farahani , "Fatigue damage and life evaluation of SS304 and Al 7050-T7541 alloys under various multiaxial strain paths by means of energy-based Fatigue damage models," Mechanics of Materials, vol. 98, pp.59–70, 2016.
[28] K.S. Kim, J.C. Park and J.W. Lee. "Multiaxial fatigue under variable amplitude loads," Journal of Engineering Materials and Technology, Trans ASME, vol. 121, pp. 286–93, 1999.
[29] J. Hoffmeyer, R. Döring, T. Seeger and M.Vormwald, "Deformation behaviour, short crack growth and fatigue lives under multiaxial nonproportional loading," International Journal of Fatigue, vol. 28, pp. 508–20, 2006.

★★★